Aristillus: the unusual narrow ribbon of dark material. B. Fitz-Gerald[1] and R. Lena[2] – BAA Lunar Section. [1] 79 South Court Ave, Dorchester, Dorset, DT12DA United Kingdom barryfitz_gerald@hotmail.com;[2] via Cartesio 144, sc. D, 00137 Rome, Italy;gibbidomine@libero.it

Introduction: Aristillus is a lunar crater that lies at the southeast of Mare Imbrium. Along the eastern inner wall and rim is an unusual narrow ribbon of dark material visible as two dark rays (of V shape) at the inner and outer slopes of the northeastern part of the crater (Fig. 3a). We attempt to define and map the rock/ mineral composition of the Aristillus crater and its two dark rays and view results in the context of local stratigraphic relationships.

Stratrigrapic relations: It is likely that Aristillus originated in a low angle but not grazing impact with the impactor arriving from the south-west. Evidence for this can be seen in the distribution of ejecta in the crossrange direction north-east and south-east to form a 'butterfly wing' pattern of enhanced secondary crater chains (Fig. 1). The downrange direction to the north-east is characterised by two prominent isolated chains of secondary craters which pass either side of the crater Theaetetus with proximal ejecta including regolith covered lower albedo impact melt streams in between [1].

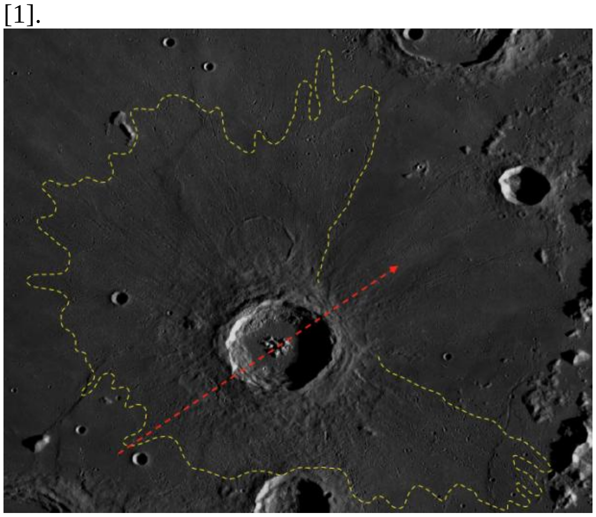

Fig. 1. WAC image of Aristillus showing approximate distribution of secondary crater chains (yellow dashed line) and inferred trajectory (red dashed line) of impactor. Downrange direction is to the NE.

The location of the V shaped dark ray appears therefore to be orientated in the downrange direction, possibly as a result of the geometry of the oblique impact event.The ray is approximately 30 kms long from its apparent origin at the base of the north-eastern crater wall. The lowermost part of the ray is however in all probability obscured by the impact melt deposits which occupy the crater floor, therefore the total length is likely to be greater. The ray splits into two some 8.5 kms from its origin, with the western arm being wider (approx 1.3 kms) than the eastern. The crater wall has a slope of approximately 13° at this location but the cause of the divergence of the eastern and western components is not obvious. The most likely explanation is blocking of the the ray by a slightly elevated topography in its path, giving rise to a shadow effect downrange. The ray appears to overlie the inner crater wall deposits, the crater rim and proximal ejecta forming the glacis of the crater in the north-east. It also appears to overlie impact melt pools that formed within topographic lows of the proximal ejecta on the north-eastern glacis. This is indicative of an origin during a late stage in the crater forming process and after the most proximal ejecta had been emplaced. This implies that the material forming the ray was excavated from the deepest part of the transient cavity.

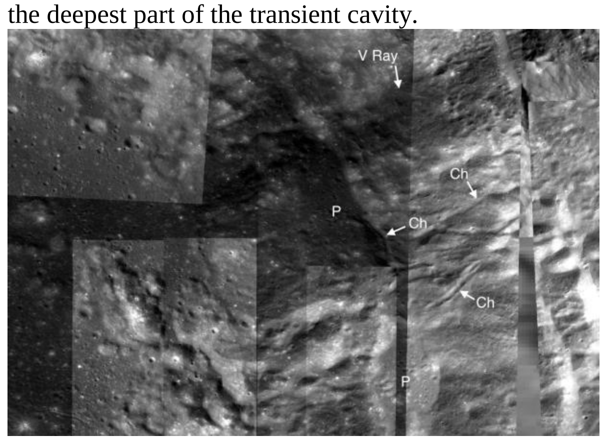

Fig. 2. NAC image mosaic of Aristillus NE crater wall showing the lower section of the V Ray, melt ponds contained within terraces (P) and impact melt channels (Ch) draining into these melt ponds.

The inner crater walls adjacent to the V ray show evidence of channels in excess of 100m wide along which impact melt has drained down from the upper slopes towards the crater floor (Fig. 2). These channels can also be seen to terminate in melt ponds which have accumulated within terraces along the inner crater wall. These areas are mineralogically distinct from and of a higher albedo than the dark ray. A possible interpretation which accounts for the composition and morphology of the V ray would be the excavation of a localised, deep seated mafic or ultramafic igneous intrusion during the very latest phase of crater excavation. The orientation of the ray would be influenced by the low angle geometry of the impact in the downrange direction.

Spectral data: The dark rays under examination, orange in the Clementine color ratio image, are characterized by an absorption trough with a minimum at 980-1030 nm, a full width at half maximum (FWHM) in the range of 240-295 nm and with a trough depth of about 7 to 9.5 %. The central peak is characterized by an absorption trough with a minimum of 940 nm, a FWHM of 235 nm, which is due to pyroxene of low Ca content, and with a trough depth of 13.4 % (indicating a more mafic content). The analysis based only on five band UVVIS spectral shape [2] indicates that the central peaks display a composition classified as *gabbroic noritic troctolitic anorthosite* (GNTA) type. The northern ejecta material displays a composition of an *anorthosite* type 2 (An2) characterized by higher *plagioclase feldspar* (Fig. 3g). The shape of the absorption band near 1000 nm based Chandrayaan-1's Moon Mineralogy Mapper (M^3) dataset (Fig. 3b-d), include for the dark rays a combination of bands of high-calcium pyroxene including Fe-rich glass, and thus consistent with an impact melt. The shallow band centered near 1270 nm is due to the feldspar absorption. We exclude the presence of admixed olivine based on Diviner Lunar Radiometer dataset where the CF displays values greater than 8.6 µm in case of olivine abundances (Fig, 3f). Previous spectra of Aristillus have been reported in [3] using an infrared spectrometer and the 2.2 m telescope of Mauna Kea observatory. Based on the metod described in [4] the abundances of the elements Ca, Al, Fe, Mg, Ti, and O were estimated (cfr. Fig. 1e). Using an analogous method defined by certain Al, Mg and Fe elemental abundance ranges it is possible to produce mineral maps for FAN (ferroan anorthositic norite), norite, dunite, gabbronorite, troctolite, mare basalt, aluminous basalt, anorthosite. The gabbronorite composition, identified in several locations of the central peaks, is reported in Fig. 1h (white colour). The ejecta material scattered over the surface of the adjacent mare of highland composition, corresponding to FAN, is indicates by the deep red color (Fig. 3h).

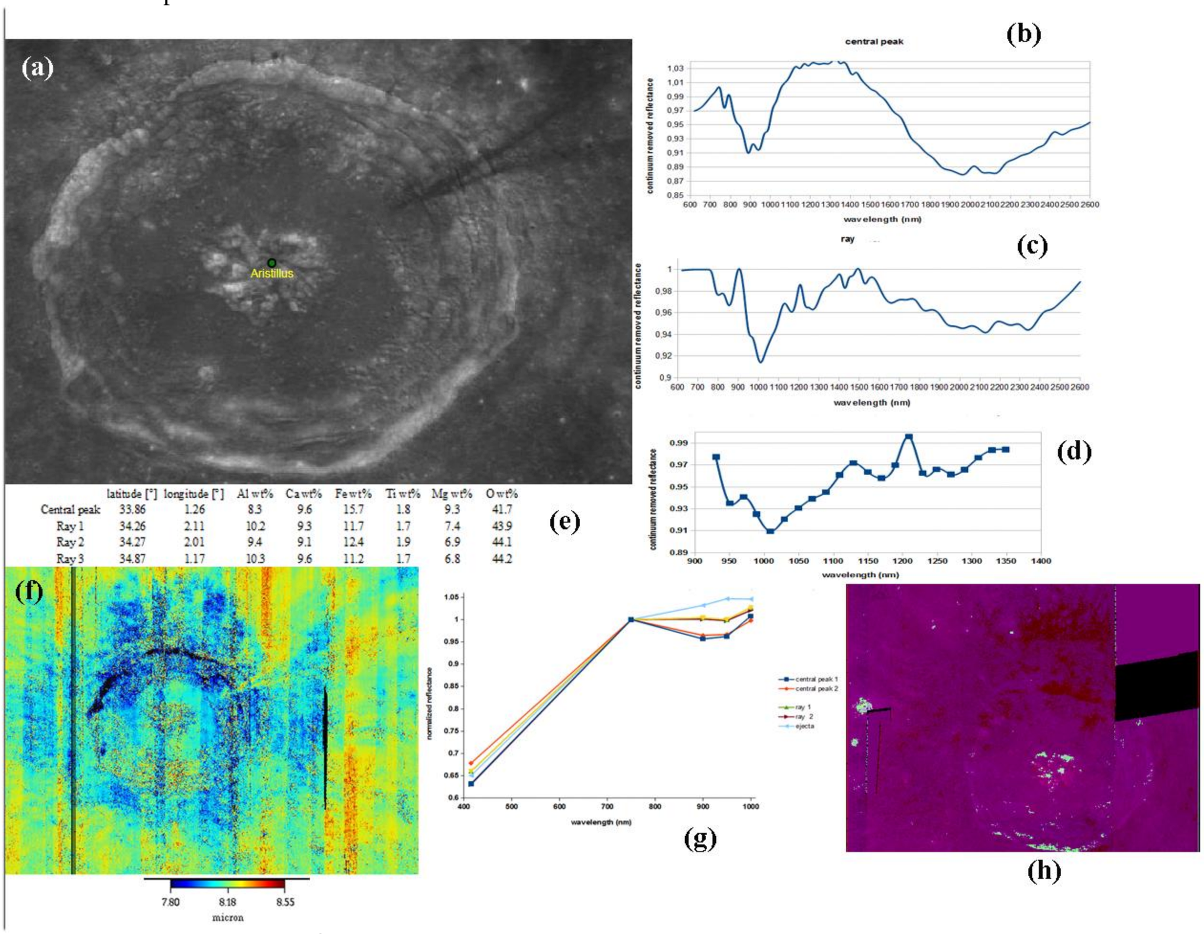

(e)

	latitude [°]	longitude [°]	Al wt%	Ca wt%	Fe wt%	Ti wt%	Mg wt%	O wt%
Central peak	33.86	1.26	8.3	9.6	15.7	1.8	9.3	41.7
Ray 1	34.26	2.11	10.2	9.3	11.7	1.7	7.4	43.9
Ray 2	34.27	2.01	9.4	9.1	12.4	1.9	6.9	44.1
Ray 3	34.87	1.17	10.3	9.6	11.2	1.7	6.8	44.2

Fig. 3. (a) WAC imagery, (b-c) M^3 spectra,orbital period OP2C1, of central peak and dark rays, (d) dark rays spectrum in wavelengths interval comprised from 920 nm to 1380 nm, (e) elemental abundances wt%, (f) Diviner LRE CF values, (g) Clementine five band UVVIS Spectra, (h) mineral map.

References: [1] Carter et al. (2012). *J. Geophys. Res.*, 117, E00H09, doi:10.1029/2011JE003911; [2] Tompkins and Pieters (1999). Meteoritics and Planetary Science, 34, 25-41; [3] Smrekar and Pieters (1999). LPI, 15, 802 S; [4] Wöhler, et al. (2011). Planetary and Space Science, vol. 59, 1, pp. 92-110.